9230 *Macromolecules* **2010**, *43*, 9230–9233
DOI: 10.1021/ma1019285

Macromolecules
COMMUNICATION TO THE EDITOR

Patterning of a Butyl Rubber−Poly(ethylene oxide) Graft Copolymer Revealed by Protein Adsorption

Colin V. Bonduelle[†] and Elizabeth R. Gillies*[,†,‡]

[†]*Department of Chemistry, The University of Western Ontario, 1151 Richmond St., London, Canada N6A 5B7, and* [‡]*Department of Chemical and Biochemical Engineering, The University of Western Ontario, 1151 Richmond St., London, Canada N6A 5B9*

Received August 20, 2010
Revised Manuscript Received October 10, 2010

The patterning of polymers on materials at different length scales is important for research fields including cell biology, tissue engineering, medical science, optics, and electronics. Macromolecular patterning can be achieved by following a bottom-up approach through phase separation during thin film formation.[1−3] Solvent-assisted deposition is often used, and three major types of interactions are involved in the pattern formation: molecule−molecule, molecule−solvent, and molecule−substrate interactions.[4] These interactions are often weak, and the morphologies of the resulting films are not always easy to predict. Thermodynamically driven organizations are generally obtained with relatively low-molecular-weight (MW) macromolecules, which often lead to nanometric surface patterning.[4] In marked contrast, the casting of high-MW polymers can create kinetically governed organizations that lead to micrometric surface patterning.[4]

Many studies have been conducted using blends of two or three polymers.[5−7] The morphologies obtained from these different blends by using solvent or temperature annealing as well as their resulting behaviors are now well understood. Patterns of linear diblock and triblock copolymers are also well characterized.[8,9] While comblike or graft copolymer architectures have provided access to interesting spherical, hexagonal cylindrical, lamellar, flower, and hyperbranched micellar morphologies after solution casting,[10−12] in general, there are relatively few examples involving these more complicated polymer architectures and their assemblies are less well understood.[13] Herein, we report the preparation of butyl rubber−poly(ethylene glycol) (PEG) graft copolymers using a new mild and clean functionalization approach. We then use fluorescent protein adsorption as a method to reveal novel complex patterns obtained by spin-casting.

A grafting-onto[14−20] or grafting-from[21] approach was previously used to introduce PEG and other polymer chains along the butyl rubber backbone via the halogenated rubber. However, these reactions involved halide substitution, a reaction that typically proceeds at high temperatures and results in the formation of multiple products. Here, butyl rubber (**1**) containing 2.2% isoprene units, with a weight-average molecular weight (M_w) of 400 000 g/mol, was used as the starting material for a mild and clean reaction sequence. As shown in Scheme 1, the double bonds of the isoprene units were converted to epoxides[22,23] using *m*-chloroperoxybenzoic acid. Next, the epoxidized butyl rubber (**2**) was reacted with catalytic HCl in toluene to cleanly afford an unexpected ring-opened product **3**. Interestingly, despite carrying the reaction out at ambient temperature, the acidic ring-opening of the epoxide was followed by alkene formation, apparently the result of an elimination reaction. However, in contrast to Saytzeff's rule, the less substituted alkene was formed (see Supporting Information for analysis). The unexpectedly clean conversion of the epoxides to hydroxyl groups along the butyl rubber backbone was then exploited to introduce activated carbonates (Scheme 1) by the reaction of polymer **3** with 4-nitrophenyl chloroformate. The reaction proceeded with complete conversion to provide **4**. This activated polymer was reactive enough to graft PEG monomethyl ether (m-PEG) with a molecular weight of 2000 g/mol (degree of polymerization ≈44) via substitution of the 4-nitrophenol leaving groups, affording graft copolymer **5**. Analysis of ^{1}H NMR spectra indicated that 16% of the isoprene units of **5** were functionalized in this final step, corresponding to a polymer comprising 8 wt % PEG.

Copolymer **5** was used to create a thin film on a silicon wafer by spin-casting a CH_2Cl_2 solution with a concentration of 8 mg/mL. The resulting film was first characterized by atomic force microscopy (AFM). This technique revealed that although the entire surface was coated with polymer, the topography was inhomogeneous, with hills and valleys associated with a roughness of 29 nm (Figure 1). However, the dimensions of the morphology were clearly larger than the limits of a standard AFM image. Related work in our laboratory has revealed that while proteins readily adsorb to butyl rubber surfaces, PEG-coated butyl surfaces resist protein adsorption, a well-known PEG phenomenon.[24] Therefore, the possibility of using the resistance of PEG to protein adsorption as a means of imaging the surface was investigated. The use of fluorescence microscopy was previously used to reveal selective protein adsorption on different morphologies for protein microarray applications.[25,26] However, to the best of our knowledge, our work is the first attempt to use this technique to access information on the patterning of a polymeric material after thin film formation. A rhodamine−fibrinogen conjugate was prepared, and the surfaces were immersed in a 3 μM solution of the labeled protein. The surfaces were then washed and imaged by fluorescence confocal microscopy.

Following protein adsorption, the surface revealed a regular pattern of fluorescent loops (Figure 2a). The importance of the copolymer was demonstrated by comparison to a blend of butyl rubber with PEG that was spin-cast at the same concentration. The covalent PEG grafting was crucial to obtain the complex pattern as the blend revealed more uniform, low levels of fluorescence (Figure 2b). More concentrated solutions of polymer **5** (15 and 20 mg/mL) were also spin-cast, and fluorescent protein was adsorbed. Even more complex patterns of fluorescence were revealed by confocal microscopy (Figure 2c,d). All of these patterns were reproducible.

To further probe the nature of the patterns, they were also imaged by polarized optical microscopy. Excellent agreement between these images and the fluorescent protein patterns was observed, as demonstrated in Figure 3. In addition, it was possible to obtain further insight into the texture of the films by optical microscopy (Supporting Information). These results were also in agreement with the polarized optical microscopy images and combined with the AFM results suggest that the fluorescent patterns reveal aspects of the topography. Although PEO is known to resist protein adsorption,[24] the nanoscale dimensions of the individual polymer chains and their relatively low PEO content make it unlikely that the large micrometer scale regions lacking fluorescence correspond entirely to PEO. Therefore, despite the initial hypothesis that protein adsorption might simply reveal polymer phase separation, topography seems to play an important role. However, the importance of phase separation resulting

*Corresponding author. E-mail: egillie@uwo.ca.

 Published on Web 10/19/2010

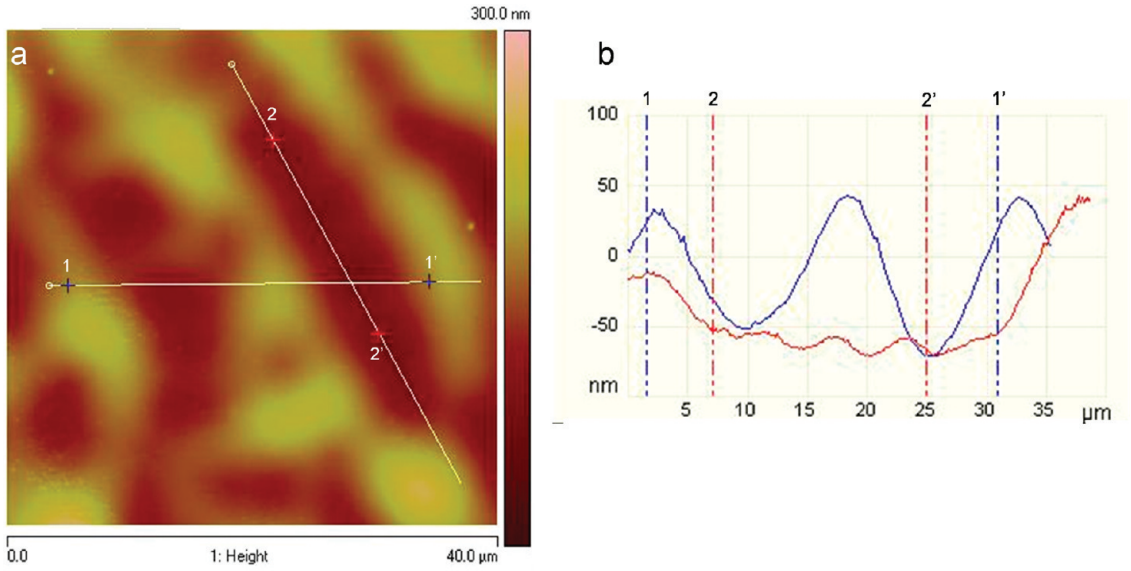

Figure 1. AFM analysis of the thin film obtained after spin-casting a solution of graft copolymer **5** (8 mg/mL in CH_2Cl_2) on a silicon wafer reveals topographical inhomogeneities. (a) Topography image. (b) Sections of the morphology.

Scheme 1. Synthesis of Butyl Rubber−PEG Graft Copolymers

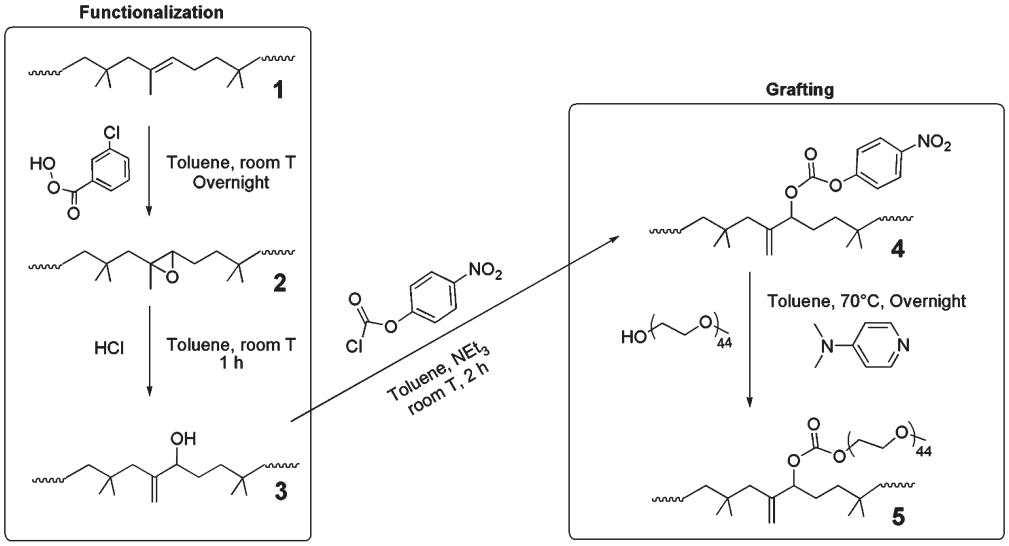

in butyl-enriched and PEO-enriched domains that can influence both the topography and the protein adsorption cannot be excluded. For example, fibrinogen has been shown previously to adsorb preferentially at the interface between two materials.[27]

The complex patterns formed by polymer **5** can potentially arise from kinetic and thermodynamic effects. It is known that after drop deposition the different interfaces of the system create a destabilized layer with a high surface roughness.[28] Roughness tends to decrease during solvent evaporation until the thin layer is formed. Solvent plays a crucial role during the step involving the leveling of the surface roughness,[29] and in the case of solvent-rich films, rapid evaporation can freeze states of the destabilized layer created by Marangoni instabilities.[30] AFM analyses of the obtained patterns indicated that the roughness of the surface was 29 nm for the sample spin-cast at 8 mg/mL, 48 nm for the sample at 15 mg/mL, and 95 nm for the sample at 20 mg/mL (Supporting Information). This significant roughness evolution at different concentrations is in agreement with a kinetic freezing of a destabilized solvent-rich layer.[29] In addition, unlike films cast from CH_2Cl_2, films cast in the same manner from hexane did not reveal regular patterns of fluorescence (Supporting Information). This can be explained by the lower vapor pressure of hexane relative to CH_2Cl_2.[29]

On the other hand, previous work has revealed phase separation of butyl rubber−PEG graft copolymers following 48 h of casting from toluene.[15] X-ray scattering (SAXS) and dynamic mechanical analyses suggested that the copolymer underwent phase separation, resulting in domains of PEG separated by distances of 100−200 nm. Consequently, it is reasonable to suggest that phase separation also played some role during spin-casting. However, the micrometer scale of the current patterns suggests a different mechanism for pattern formation and lends support to the hypothesis that kinetic factors also play an important role. Furthermore, the average film thicknesses increased with increasing polymer concentration (135 nm for 8 mg/mL, 159 nm for 15 mg/mL, and 263 nm for 20 mg/mL), and this could also change the relative importance of the different interfacial energies of the system. Thus, a combination of both kinetic and thermodynamic aspects was likely involved in the patterning process.

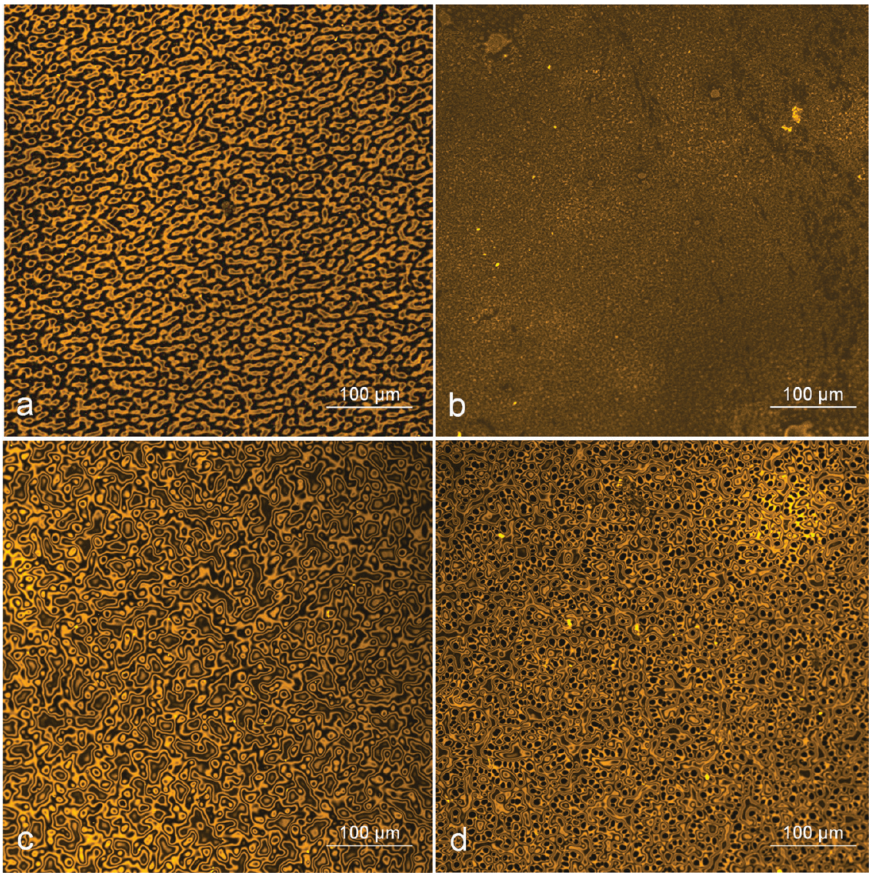

Figure 2. Fluorescence confocal microscopy images (543 nm) of thin films following adsorption of a rhodamine−fibrinogen conjuguate: (a) polymer **5** spin-cast at 8 mg/mL; (b) blend of PEG/butyl rubber (containing 8 wt % PEG); (c) polymer **5** spin-cast at 15 mg/mL; (d) polymer **5** spin-cast at 20 mg/mL. These images reveal the importance of the covalent graft copolymer in the pattern formation and the evolution of patterns with polymer concentration.

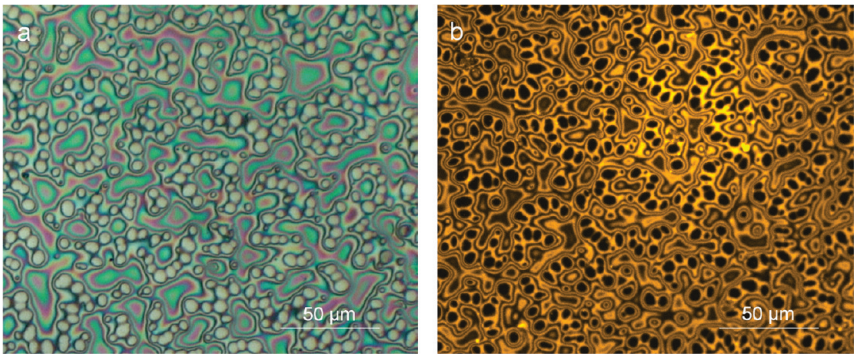

Figure 3. A thin film of copolymer **5** spin-cast at 20 mg/mL and imaged by (a) polarized optical microscopy and (b) confocal fluorescence microscopy (543 nm) following the adsorption of a fluorescent rhodamine−fibrinogen conjugate. Similar patterns were observed by both techniques.

In summary, a new mild and clean synthetic approach was used to prepare a butyl rubber−PEG graft copolymer. The micrometric patterning of this polymer during thin film formation was studied by optical microscopies and by imaging the adsorption of a fluorescently labeled protein. Although the exact nature of the protein adsorption is still not fully understood, these results demonstrate for the first time that protein adsorption is a useful tool to study complex pattern formation in thin films of polymers. Furthermore, patterns were not obtained using simple blends of butyl rubber and PEO, highlighting the importance of the graft copolymer in promoting the formation of the complex patterns. It is proposed that these patterns were created by a combination of kinetic and thermodynamic effects, mainly the freezing of instabilities formed during the thin film formation as well as polymer phase separation. A more detailed study of the nature of each pattern and the effect of the PEG composition and molecular weight is currently underway in our laboratory. Moreover, the use of our chemistry to graft other polymers and small molecules onto the butyl rubber backbone is also under investigation in order to impart new properties.

Acknowledgment. We thank LANXESS Inc. for funding of this work and for providing samples of butyl rubber. The Ontario Centres of Excellence and the Natural Sciences and Engineering Research Council of Canada are also thanked for funding. Surface Science Western (Heng-Yong Nie) is thanked for assistance

with AFM imaging, and the Biotron Imaging Facility is thanked for help with optical imaging.

Supporting Information Available: Synthetic procedures and characterization data for the polymers, preparation of the thin films, AFM roughness measurements, protein adsorption and fluorescence imaging, and optical microscopy. This material is available free of charge via the Internet at http://pubs.acs.org.

References and Notes

(1) Whitesides, G. M.; Grzybowski, B. *Science* **2002**, *295*, 2418–2421.
(2) Shimomura, M.; Sawadaishi, T. *Curr. Opin. Colloid Interface Sci.* **2001**, *6*, 11–16.
(3) Nie, Z.; Kumacheva, E. *Nature Mater.* **2008**, *7*, 277–290.
(4) Palermo, V.; Samori, P. *Angew. Chem., Int. Ed.* **2007**, *46*, 4428–4432.
(5) Dalnoki-Veress, K.; Forrest, J. A.; Stevens, J. R.; Dutcher, J. R. *Physica A* **1997**, *239*, 87–94.
(6) Walheim, S.; Böltau, M.; Mlynek, J.; Krausch, G.; Steiner, U. *Macromolecules* **1997**, *30*, 4995–5003.
(7) Sprenger, M.; Walheim, S.; Budkowski, A.; Steiner, U. *Interface Sci.* **2003**, *11*, 225–235.
(8) Darling, S. B. *Prog. Polym. Sci.* **2007**, *32*, 1152–1204.
(9) Hamley, I. W. *Prog. Polym. Sci.* **2009**, *34*, 1161–1210.
(10) Kishida, A.; Seto, F.; Hiwatari, K.; Serizawa, T.; Muraoka, Y.; Akashi, M. *Chem. Lett.* **1999**, 1221–1222.
(11) Ruokolainen, J.; Saariaho, M.; Ikkala, O. *Macromolecules* **1999**, *32*, 1152–1158.
(12) Lanson, D.; Schappacher, M.; Borsali, R.; Deffieux, A. *Macromolecules* **2007**, *40*, 9503–9509.
(13) van Zoelen, W.; Ten Brinke, G. *Soft Matter* **2009**, *5*, 1568–1582.
(14) Yamashita, S.; Kodama, K.; Ikeda, Y.; Kohjiya, S. *J. Polym. Sci., Part A: Polym. Chem.* **1993**, *31*, 2437–2444.
(15) Ikeda, Y.; Kodama, K.; Kajiwara, K.; Kohjiya, S. *J. Polym. Sci., Part B: Polym. Phys.* **1995**, *33*, 387–394.
(16) Guillen-Castellanos, S. A.; Parent, J. S.; Whitney, R. A. *J. Polym. Sci., Part A: Polym. Chem.* **2006**, *44*, 983–992.
(17) McLean, J. K.; Guillen-Castellanos, S. A.; Parent, J. S.; Whitney, R. A.; Resendes, R. *Eur. Polym. J.* **2007**, *43*, 4619–4627.
(18) Guillen-Castellanos, S. A.; Parent, J. S.; Whitney, R. A. *Macromolecules* **2006**, *39*, 2514–2520.
(19) McLean, J. K.; Guillen-Castellanos, S. A.; Parent, J. S.; Whitney, R. A.; Kulbaba, K.; Osman, A. *Ind. Eng. Chem. Res.* **2009**, *48*, 10759–10764.
(20) Parent, J. S.; Malmberg, S.; McLean, J. K.; Whitney, R. A. *Eur. Polym. J.* **2010**, *46*, 702–708.
(21) Dreyfuss, P.; Kennedy, J. P. *Appl. Polym. Symp.* **1977**, *30*, 165–178.
(22) Jian, X.; Hay, A. S. *J. Polym. Sci., Part A: Polym. Chem.* **1991**, *29*, 547–553.
(23) Puskas, J. E.; Wilds, C. *Rubber Chem. Technol.* **1994**, *67*, 329–341.
(24) Andrade, J. D.; Hlady, V.; Jeon, S. I. *Adv. Chem. Ser.* **1996**, *248*, 51–59.
(25) Lau, K. H. A.; Bang, J.; Hawker, C. J.; Kim, D. H.; Knoll, W. *Biomacromolecules* **2009**, *10*, 1061–1066.
(26) Zemła, J.; Lekka, M.; Raczkowska, J.; Bernasik, A.; Rysz, J.; Budkowski, A. *Biomacromolecules* **2009**, *10*, 2101–2109.
(27) Morin, C.; Hitchcock, A. P.; Cornelius, R. M.; Brash, J. L.; Urquhart, S. G.; Scholl, A.; Doran, A. *J. Electron Spectrosc. Relat. Phenom.* **2004**, *137−140*, 785–794.
(28) Heriot, S. Y.; Jones, R. A. L. *Nature Mater.* **2005**, *4*, 782–786.
(29) Strawhecker, K. E.; Kumar, S. K.; Douglas, J. F.; Karim, A. *Macromolecules* **2001**, *34*, 4669–4672.
(30) Scriven, L. E.; Sternling, C. V. *Nature* **1960**, *187*, 186–188.